

Magnetic Nanoclusters for Ultrasensitive Magnetophoretic Assays**

Zongwen Jin, Young Ki Hahn, Eunkeu Oh, Young-Pil Kim, Je-Kyun Park,*
Seung Ho Moon, Jung-Tak Jang, Jinwoo Cheon, and Hak-Sung Kim*

Assays of metabolites and disease biomarkers with high sensitivity are most demanding in the fields of medical and biological sciences. To accomplish this goal, the use of magnetic particles (MPs) has been attractive mainly due to their distinct advantages, including facile control by magnetism, high biocompatibility, and high detection sensitivity.^[1–7] In particular, integration with microfluidic systems endowed the MP-based assay with significantly enhanced sensitivity and selectivity in detecting target analytes.^[8,9] In addition to the combination of a microfluidic system, modulations in the structure and shape of MPs are expected to confer enhanced analytical performance on the MP-based assay. It was reported that multimeric form or self-assembly of magnetic nanoparticles (MNPs) can improve the sensitivity of the bioassay due to the amplified transverse relaxation time.^[10]

We recently demonstrated a magnetophoretic assay platform using the MNPs in a microfluidic channel.^[11,12] However, to broaden the utility of the developed system for the assay of analytes with low abundance, a more sensitive approach remains to be developed. Here we report on the construction of magnetic nanoclusters (MNCs) and their use for the development of an ultrasensitive magnetophoretic assay system as a signal amplifier. As a target analyte, prostate-specific antigen (PSA) was employed. PSA is recently recognized as a potential biomarker for breast cancer.^[13,14] The PSA level in female serum ($<40 \text{ pg mL}^{-1}$) is about three orders of magnitude lower than in male, and its detection using conventional methods might be difficult.^[15]

The magnetophoretic assay system using MNCs is depicted in Scheme 1. Monoclonal anti-PSA antibody is immobilized on microbeads, and magnetic nanoparticles are modified with both neutravidin and polyclonal anti-PSA antibody. MNCs are constructed by reacting the dually modified magnetic nanoparticles (DMNPs) with biotinylated bovine serum albumin (BSA). Microbeads are incubated with a sample solution containing PSA followed by reaction with the MNCs. The resulting MNC-associated microbeads are flowed into a microfluidic channel under a magnetic field, and their deflection

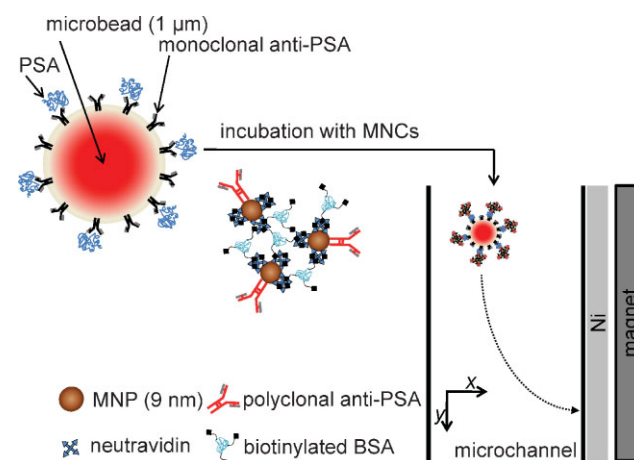
[*] Prof. H.-S. Kim
Department of Biological Sciences and
Graduate school of Nanoscience & Technology
KAIST
Daejeon 305–701 (Korea)
E-mail: hskim76@kaist.ac.kr
Z. Jin,^[+] Dr. E. Oh, Dr. Y.-P. Kim
Department of Biological Sciences
KAIST
Daejeon 305–701 (Korea)
Prof. J.-K. Park, Y. K. Hahn^[+]
Department of Bio and Brain Engineering
KAIST
Daejeon 305–701 (Korea)
E-mail: jekyun@kaist.ac.kr
Prof. J. Cheon, J.-T. Jang, S. H. Moon
Department of Chemistry
Yonsei University
Seoul, 120–749 (Korea)

[+] These authors equally contributed to this work.

[**] This research was supported by the Nano/Bio Science and Technology Program (2005-01291), Nano-Science & Technology Program (M10503000868-08M0300-86810), Pioneer Research Program for Converging Technology (M10711300001-08M1130-00110), WCU program (R31-2008-000-10071-0), Brain Korea 21 of MEST, and the Korea Health 21C R&D Project (A04-0041-B21004-08A5-00030B) of MIHWAF.

Supporting Information is available on the WWW under <http://www.small-journal.com> or from the author.

DOI: 10.1002/sml.200900311



Scheme 1. Magnetophoretic assay system using MNCs. PSA is captured by anti-PSA antibody on a microbead, and the resulting microbead is incubated with MNCs for magnetic labeling. The MNC-associated microbead is subjected to injection into a microfluidic channel under a magnetic-field gradient, and its deflection velocity toward the x axis is determined.

velocities are determined to correlate them with the PSA concentration.

The deflection velocity of a microbead is proportional to the total number of associated magnetic nanoparticles, which will be most critically affected by the size of MNCs. When considering the mechanism by which MNCs are formed between biotinylated BSA and the DMNPs, the size of MNCs will vary with the ratio of the DMNP to the biotinylated BSA. To investigate the effect of the ratio on the deflection velocity of a microbead, biotinylated BSA and the DMNP were mixed at different ratios, incubated for 30 min, followed by the addition of excess D-biotin to prevent further growth of MNCs. The resulting MNCs formed at different ratios were used for magnetophoretic assays. As a result, the deflection velocity of a microbead was found to increase with the increasing ratio, approaching a maximum at the molar ratio of 1:100 (DMNP:BSA) (Figure 1).

To get more detailed information on the size of the MNCs formed at the above ratio, we attempted to estimate the average size of the MNCs by using transmission electron microscopy (TEM). Given that the degree of biotinylation of BSA and the amounts of neutravidin and anti-PSA antibody on each magnetic nanoparticle are fixed, the MNCs are expected to have a size distribution in solution. We constructed the MNCs according to the procedure described above, and examined their TEM images. The formation of MNCs was clearly observed, and their size and shape were found to vary mainly due to random morphology of clusters. From the TEM images of MNCs, the size of MNCs ranged from 60 nm to 80 nm, and the average number of MNPs per each MNC was estimated to be 18 ± 5 ($n = 17$) at 24 h after the addition of D-biotin. No aggregates were observed in the absence of biotinylated BSA (Figure 2).

To further confirm the formation of MNCs in a time-course manner, the changes in the T2 relaxation time of MNCs were directly measured in solution at intervals after the addition of D-biotin (Figure 3). The T2 relaxation time of the MNCs was revealed to decrease at about 30 min of incubation after the addition of D-biotin, even though the total concentration of

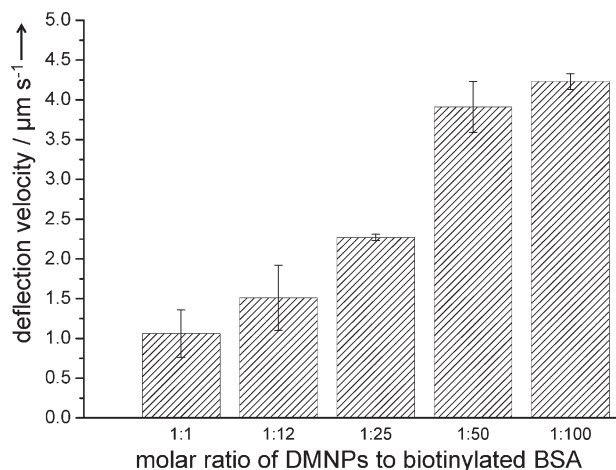


Figure 1. Average deflection velocities of microbeads using MNCs formed at different ratios. The concentration of PSA was fixed at 10 pg mL^{-1} . Assay was repeated three times, and the error bars represent the standard deviation of the assay.

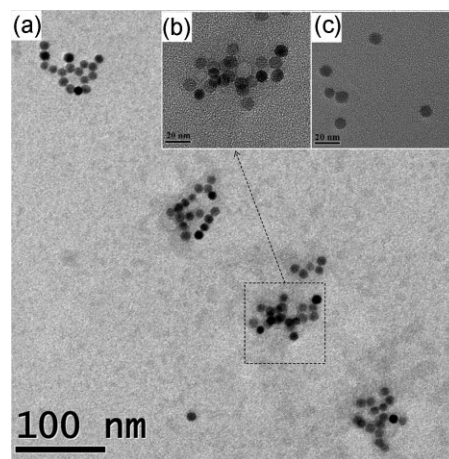


Figure 2. a) TEM images of MNCs at 24 h. b) Zoomed image of dashed square in (a). c) DMNPs in the absence of biotinylated BSA.

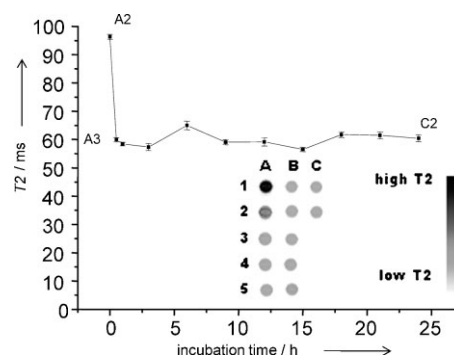


Figure 3. T2 relaxation times of MNCs at different incubation times after addition of D-biotin. A1: buffer only, A2: DMNPs, A3: 30 min, A4: 1 h, A5: 3 h, B1: 6 h, B2: 9 h, B3: 12 h, B4: 15 h, B5: 18 h, C1: 21 h, C2: 24 h. Control experiment was carried out at the same concentration of the DMNPs in the absence of biotinylated BSA. The inset image represents an inverted grayscale image of the one originally obtained with MRI.

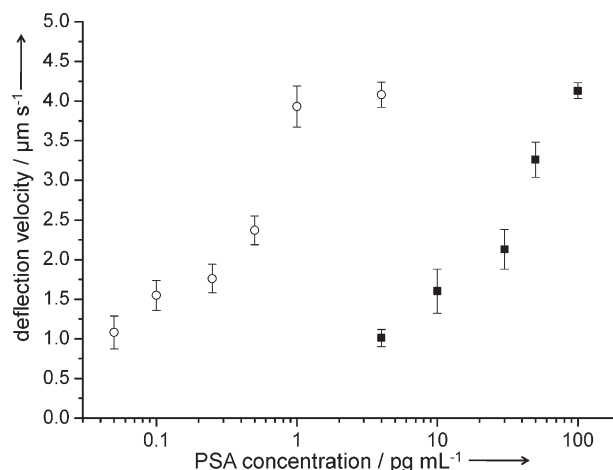


Figure 4. Average deflection velocity of microbeads at different PSA concentrations when MNCs (open circles) and DMNPs (rectangles) were used. Assay was repeated three times at a specified concentration. The error bars represent the standard deviation of the assay.

MNPs in solution was the same as in the control experiment. This result indicates that the reduction of T2 relaxation time was caused by the co-operative magnetic interactions as MNPs are clustered,^[16,17] clearly showing formation of MNCs in the presence of biotinylated BSA. In addition, no noticeable change in T2 relaxation time was observed during subsequent incubation until 24 h. This result shows that D-biotin was effective in preventing MNCs from further aggregation by blocking the biotin binding sites on the DMNPs.

With the optimized MNCs, magnetophoretic assay of PSA was conducted. For comparison, deflection velocity of a microbead was also determined using the DMNPs alone instead of MNCs. When the DMNPs were used, the background velocity in the absence of PSA was estimated to be $0.86 \pm 0.2 \mu\text{m s}^{-1}$. On the other hand, when MNCs were used in buffer solution, the background velocity was lowered to $0.16 \pm 0.2 \mu\text{m s}^{-1}$. To correlate the deflection velocity of a microbead with PSA concentration, we averaged the deflection velocities of around 15 microbeads at specified PSA concentration. As a result, the microbead velocity increased in proportional to the concentration of PSA up to 1.0 pg mL^{-1} from a level as low as 50 fg mL^{-1} above the background, which is a favorable range for detecting female PSA with low abundance^[18] (Figure 4). When the DMNPs were employed, however, a dynamic range varied from 4 to 100 pg mL^{-1} , even though a similar pattern was observed. The detection limit of the magnetophoretic assay using MNCs was estimated to be 45 fg mL^{-1} according to a method reported elsewhere,^[19] and this is two orders of magnitude lower than that of using the DMNPs ($\approx 8 \text{ pg mL}^{-1}$). Interestingly, maximum average velocities for the assays using either MNCs or the DMNPs were almost similar, reaching about $4 \mu\text{m s}^{-1}$. This can be explained by the limited binding capacity of the microbead for MNPs. The deflection velocity of a microbead is proportional to the total number of bound magnetic nanoparticles. Thus, when DMNPs were employed, the deflection velocity of microbeads became detectable at relatively high concentrations of PSA. On the other hand, in the case of MNCs, the binding of MNCs might be much more effective for lower levels of PSA due to larger size of MNCs, which resulted in a significant deflection velocity even at low PSA levels.

In conclusion, we have demonstrated construction of the MNCs and their use in an ultrasensitive magnetophoretic assay system as an effective signal amplifier. The developed system enabled detection of PSA as low as 50 fg mL^{-1} with a detection limit of 45 fg mL^{-1} . It is anticipated that the present assay format will find applications in the detection of target analytes including disease biomarkers with low abundance.

Experimental Section

Materials: Stock solution contained $28 \mu\text{g mL}^{-1}$ PSA in PBS buffer (pH 7.4) containing 0.1% BSA. Each standard PSA solution with different concentrations was prepared by serial dilution of the stock solution with PBS buffer (pH 7.4, 0.1% BSA). Conjugation of antibody to microbeads, synthesis of DMNPs, and preparation of MNCs are described in the Supporting Information.

TEM images of DMNPs and MNCs: A field-emission source

transmission electron microscope (JEOL JEM-2100F) was used to obtain the images of DMNPs and MNCs. A 300-mesh carbon-coated grid was pre-treated with 0.2 mg mL^{-1} bacitracin solution for 90 s, immediately removed from solution, and put into the paraffin film. Each solution of DMNPs and MNCs containing the same concentration of magnetic nanoparticles was dropped onto a carbon grid and incubated for 90 s. After incubation, the solutions were immediately removed using a filter paper on rims of grids. Carbon grids were dried out at room temperature for 60 min, and subjected to TEM imaging. The acquired TEM images were used to estimate the number of MNPs per single MNC.

Measurement of MR contrast effect of MNCs: MRI was performed with a 4.7 T BioSpin MRI with a 72-mm microcoil (Bruker, Billerica, MA). At room temperature, T2-weighted MR images of various MNCs samples were measured. The following parameters were used: fast spin-echo mode, point resolution of $469 \mu\text{m} \times 469 \mu\text{m}$, section thickness = 2.0 mm, echo time TE = 2.878, 14.39, 29.78, 48.10, 66.19, 83.46, 103.61, 118.00, 132.39, 146.78, 161.17, 75.56, 189.95, 204.34 ms, repetition time TR = 5000 ms, number of acquisition = 1.

Magnetophoretic assay of human PSA: For magnetophoretic assay of PSA using MNCs, $5 \mu\text{L}$ of microbeads (approximately 5.7×10^4 beads) conjugated with monoclonal anti-PSA was mixed with $65 \mu\text{L}$ of reaction buffer ($1 \times \text{PBS}$, 0.5 M NaCl, 0.02% Tween 20, pH 7.4), and briefly vortexed and sonicated for 15 s. The PSA solution ($10 \mu\text{L}$) was added to the solution containing microbeads and incubated at room temperature for 10 min. After incubation, a solution containing MNCs was added and further incubated for 10 min. The resulting solution was injected into a microfluidic channel to measure the deflection velocities of microbeads. For comparison, the DMNPs were used instead of MNCs according to the same procedure. Following injection into the microfluidic device, the movements of around 15 microbeads were recorded to measure their velocities. By using statistical analysis, the average velocity and standard deviation were calculated, and velocities of microbeads within the range of $V_{\text{avg}} \pm \sigma$ were again averaged. V_{avg} and σ represent the average microbead velocity and standard deviation in the first measurement, respectively. The mean velocity from triplicate assays at different PSA concentrations was used to obtain a correlation curve.

Keywords:

magnetic nanoclusters · magnetophoretic assays · magnetic nanoparticles · microfluidics

- [1] N. Pamme, *Lab Chip* **2006**, *6*, 24–38.
- [2] A. Ito, M. Shinkai, H. Honda, T. J. Kobayashi, *Biosci. Bioeng.* **2005**, *100*, 1–11.
- [3] C. Zhang, B. Wängler, B. Morgenstern, H. Zentgraf, M. Eisenhut, H. Untenecker, R. Krüger, R. Huss, C. Seliger, W. Semmler, F. Kiessling, *Langmuir* **2007**, *23*, 1427–1434.
- [4] S. Sun, S. Anders, H. F. Hamann, J. U. Thiele, J. E. Baglin, T. Thomson, E. E. Fullerton, C. B. Murray, B. D. Terris, *J. Am. Chem. Soc.* **2002**, *124*, 2884–2885.
- [5] C. R. Tamaha, S. P. Mulvaney, J. C. Rife, L. J. Whitman, *Biosens. Bioelectron.* **2008**, *24*, 1–13.
- [6] W. B. Tan, Y. Zhang, *Adv. Mater.* **2005**, *17*, 2375–2380.
- [7] J. M. Perez, T. O'Loughin, F. J. Simeone, R. Weissleder, L. Josephson, *J. Am. Chem. Soc.* **2002**, *124*, 2856–2857.
- [8] M. A. M. Gijs, *Microfluid. Nanofluid.* **2004**, *1*, 22–40.

- [9] J. W. Choi, K. W. Oh, J. H. Thomas, W. R. Heineman, H. B. Halsall, J. H. Nevin, A. J. Helmicki, H. T. Henderson, C. H. Ahn, *Lab Chip* **2002**, *2*, 27–30.
- [10] G. Von Maltzahn, T. J. Harris, J. H. Park, D. H. Min, A. J. Schmidt, M. J. Sailor, S. N. Bhatia, *J. Am. Chem. Soc.* **2007**, *129*, 6064–6065.
- [11] K. S. Kim, J. K. Park, *Lab Chip* **2005**, *5*, 657–664.
- [12] Y. K. Hahn, Z. Jin, J. H. Kang, E. Oh, M. K. Han, H. S. Kim, J. T. Jang, J. H. Lee, J. Cheon, S. H. Kim, H. S. Park, J. K. Park, *Anal. Chem.* **2007**, *79*, 2214–2220.
- [13] E. P. Diamandis, H. Yu, D. J. Sutherland, *Breast Cancer Res. Treat.* **1994**, *32*, 301–310.
- [14] D. N. Melegos, E. P. Diamandis, *Clin. Chem.* **1998**, *44*, 691–692.
- [15] D. A. Healy, C. J. Hayes, P. Leonard, L. McKenna, R. O’Kennedy, *Trends Biotechnol.* **2007**, *25*, 125–131.
- [16] S. H. Koenig, K. E. Keller, *Magn. Reson. Med.* **1995**, *34*, 227–233.
- [17] Y. W. Jun, J. H. Lee, J. Cheon, *Angew. Chem. Int. Ed.* **2008**, *47*, 5122–5135.
- [18] D. N. Melegos, E. P. Diamandis, *Clin. Chem.* **1998**, *44*, 691–692.
- [19] H. Kaiser, *Anal. Chem.* **1987**, *42*, 53A.

Received: February 19, 2009
Published online: May 26, 2009